

NJC

Accepted Manuscript



This is an *Accepted Manuscript*, which has been through the Royal Society of Chemistry peer review process and has been accepted for publication.

Accepted Manuscripts are published online shortly after acceptance, before technical editing, formatting and proof reading. Using this free service, authors can make their results available to the community, in citable form, before we publish the edited article. We will replace this *Accepted Manuscript* with the edited and formatted *Advance Article* as soon as it is available.

You can find more information about *Accepted Manuscripts* in the [Information for Authors](#).

Please note that technical editing may introduce minor changes to the text and/or graphics, which may alter content. The journal's standard [Terms & Conditions](#) and the [Ethical guidelines](#) still apply. In no event shall the Royal Society of Chemistry be held responsible for any errors or omissions in this *Accepted Manuscript* or any consequences arising from the use of any information it contains.

A new Schiff base and its metal complex as a fluorescent-colorimetric sensor for rapid detection of arginine

Anupam Ghorai, Jahangir Mondal and Goutam K Patra*

Department of Chemistry, Guru Ghasidas Vishwavidyalaya, Bilaspur (C.G)

Abstract

A novel Schiff base and its Pb^{2+} -complex have been synthesised and exploited as colorimetric and fluorescent-colorimetric sensor respectively targeting the detection of arginine (Arg). Both the chemo-sensors employed here are simple, easy to synthesize and cost effective. They exhibit excellent selectivity and sensitivity towards Arg by giving dual responsive signals of visible colour change and 'on-off' fluorescence change within 1 min. The chemo-sensors having sufficiently low detection limits and rapid response time warrants their application in environmental analyses of Arg.

* *Corresponding Author*: Tel.: 91 7587312992, *E-mail*: patra29in@yahoo.co.in

Introduction

Amino acids being a class of organic compounds containing amino and carboxyl groups are not only the building blocks of biological macro-molecular proteins, but also the metabolic precursors of a variety of primary and secondary metabolites.¹ Among twenty natural amino acids, arginine has attracted considerable attention because it plays a vital role in many biological functions, e.g. cell division, healing of wounds, removal of ammonia from body, functioning of immune system, erectile dysfunction, blood vessel dilation, protein production and release of hormones etc.²⁻⁵ More over arginine is the immediate precursor of NO (a key mediator in vascular homeostasis), urea, ornithine, and agmatine.⁶⁻⁹ Having so much influence in different biological processes occurred in a human body, the presence of arginine or some arginine-derived species in too little or too much amount can be unhealthy and even life-threatening.^{10,11} Thus, arginine can be used as a possible diagnostic indicator for some diseases.¹² As a charged amino acid, arginine is the best target among the twenty amino acids for the molecular recognition of a specific side chain in a peptide.^{13,14} Hence it is of urgent need to develop feasible methods for detection of arginine with practical application. Till date, a variety of strategies for detecting arginine have been reported, for example, high-performance liquid chromatography (HPLC), liquid chromatography–tandem mass spectrometry (LC–MS) and molecular recognition technology.¹⁵⁻¹⁷ Although these approaches make great contributions to the arginine detection, most of them suffer from a number of disadvantages, such as low selectivity and sensitivity, poor precision, high costs, complexity of the equipment, complicated laboratory procedures, insufficient operating and storage stability for biosensors etc.¹⁸⁻²⁶ Therefore, the development of a simple, facile, accurate and rapid method for detecting arginine is highly desirable.

Recently, great efforts have been made to develop fluorescent chemo-sensors for detection of amino acids owing to their simplicity, high selectivity and sensitivity.²⁷⁻³⁵ In spite of these, selective detection of arginine without interference from other amino acids is a challenging task and therefore there is paucity of fluorescent chemo-sensors for arginine in literature.³⁶⁻³⁸ Recently one arginine sensor have been reported by Cao et al.³⁹ But it does not provide any privilege of naked eye visible sensing and the sensing of arginine is coupled with lysine and thus limits its selectivity for arginine. Pu et al.⁴⁰ reported a colorimetric sensor based on costly gold nano-particles. Moreover it did not show any fluorescence property.

As a part of our ongoing research^{41,42} in the design and synthesis of chemo-sensors for anions, cations and neutral molecules, we have synthesised a novel and simple azino bis-Schiff base ligand **L**. In this work, the ligand **L** and its Pb²⁺-complex, [PbL₂]²⁺ have been exploited as colorimetric and fluorescent-colorimetric chemo-sensor respectively for selective detection of arginine. The ligand exhibits change in absorbance on addition of arginine with easily discernible colour change from colourless to yellow. On the other hand Pb²⁺-complex can perform rapid sensing by quenching of fluorescence with an instantaneous colour change from yellow to colourless. To the best of our knowledge, this is the first example of a Schiff base and its metal complex acting as efficient sensors for arginine detection, which provide dual responsive signals of naked-eye visible colorimetric change and fluorescence emission change.

Experimental

General information

UV-Visible spectra were recorded on a Shimadzu UV 1800 spectrophotometer using a 10 mm path length quartz cuvette. Fluorescence spectra were recorded on a Hitachi spectrophotometer. ¹H and ¹³C NMR spectra of ligand **L** were recorded on a Bruker Ultrashield 400 using CDCl₃ and NMR spectra of Pb²⁺-complex were carried out in solvent mixture of DMSO-d₆ and D₂O respectively at room temperature and the chemical shifts are reported in δ values (ppm) relative to TMS. High resolution mass (HRMS) spectra and ESI were recorded on a Waters mass spectrometer using mixed solvent HPLC methanol and triple distilled water. All the chemicals and metal salts were purchased from Merck.

Synthesis and characterisation of **L** and [PbL₂](NO₃)₂

Benzildihydrazone (1.190 g, 5 mmol) is dissolved in 100 mL of anhydrous methanol. To this solution, 1.82 g (10 mmol) of solid syringaldehyde is added with constant stirring. The resulting bright yellowish solution is refluxed for 12h, maintaining dry condition. Then the reaction mixture is cooled to room temperature. Light yellow crystalline solid (suitable for X-ray analysis) precipitates out. It is filtered off, and dried in air. Yield, 2.35 (72%); mp, 202°C. ¹H NMR (400 MHz, CDCl₃, TMS): δ 8.30 (s, -HC=N, 2H), 7.89 (d, 4H), 7.39 (dd, 6H), 6.75 (s, 4H), 3.77 (s, -OCH₃, 12H) (Fig S1). ¹³C NMR (400 MHz, CDCl₃, δ ppm, TMS): 165.1, 159.4, 147.10, 137.8, 135.3, 130.6, 128.7, 127.7, 125.9, 105.6 and 56.4 (Fig. S2). FTIR/cm⁻¹ (KBr): 692(w), 729 (w), 756 (w), 1114(vs), 1157(m), 1216(s), 1246(m), 1317(s), 1355(s), 1421(m), 1458(s), 1512 (vs), 1597(vs, -C=N), 3408 (w) (Fig. S3). ESI MS: 567.50 (LH+,

100%) (Fig. S4). UV-VIS $\lambda_{\text{max}}/\text{nm}$ ($\epsilon/\text{dm}^3 \text{ mol}^{-1} \text{ cm}^{-1}$) (CH_3OH): 345 (40 970). Anal. Calc. for $\text{C}_{32}\text{H}_{30}\text{N}_4\text{O}_6$: C, 67.83; H, 5.34; N, 9.89. Found C, 67.77; H, 5.39; N, 9.85%.

To a methanol solution of **L** (0.566 g, 1 mmol), solid $\text{Pb}(\text{NO}_3)_2$ (0.165 g, 0.5 mmol) was added. The reaction mixture was stirred for 2 h under reflux condition. Then the reaction mixture was cooled at room temperature. A yellow solid precipitated on evaporation of the solvent, was filtered. The solid mass was washed subsequently with diethyl ether for several times and dried in air. Yield, 0.475 (65%). FTIR/ cm^{-1} (KBr): 503(w), 572 (m), 618 (w), 648(w), 690(s), 725(s) 756 (m), 1114(vs), 1157(m), 1216(s), 1246(m), 1310(vs, NO_3^-), 1363(s), 1421(m), 1440(m), 1508 (vs), 1600 (vs, $-\text{C}=\text{N}$), 3408(w) (Fig. S3). ^1H NMR (400 MHz, DMSO-d_6 , TMS): δ 9.0 (s, $-\text{OH}$, 2H), 8.32 (s, $-\text{HC}=\text{N}$, 2H), 7.75 (d, 4H), 7.41(6H), 6.70 (s, 4H), 3.67 (s, $-\text{OCH}_3$, 12H) (Fig S5). HRMS: 1339.50 ($[\text{PbL}_2]^{2+}$) (Fig. S6). UV-VIS $\lambda_{\text{max}}/\text{nm}$ ($\epsilon/\text{dm}^3 \text{ mol}^{-1} \text{ cm}^{-1}$) (CH_3OH): 340 (2950), 243 (2420). Anal. Calc. for $\text{C}_{64}\text{H}_{60}\text{N}_{10}\text{O}_{18}\text{Pb}$: C, 52.49; H, 4.13; N, 9.56. Found C, 52.45; H, 4.16; N, 9.61%.

X-ray data collection and structural determination

X-ray single crystal data were collected using $\text{MoK}\alpha$ ($\lambda = 0.7107 \text{ \AA}$) radiation on a BRUKER APEX II diffractometer equipped with CCD area detector. Data collection, data reduction, structure solution/refinement were carried out using the software package of SMART APEX.⁴³ The structures were solved by direct methods (SHELXS-97) and upgraded by using ShelXL2013 and standard Fourier techniques, and refined on F2 using full matrix least squares procedures (SHELXL-97) using the SHELX-97 package⁴⁴ incorporated in WinGX.⁴⁵ In most of the cases, non-hydrogen atoms were treated anisotropically. Hydrogen atoms were fixed geometrically at their calculated positions following riding atom model. The crystallographic data are listed in Table 1. Structural information has been deposited at the Cambridge Crystallographic Data Center (CCDC 1410686).

X-ray single crystal data were collected using $\text{MoK}\alpha$ ($\lambda = 0.7107 \text{ \AA}$) radiation on a BRUKER APEX II diffractometer equipped with CCD area detector. Data collection, data reduction, structure solution/refinement were carried out using the software package of SMART APEX.⁴³ The structures were refined using ShelXL-2013.⁴⁴ All the non-hydrogen atoms were treated anisotropically. Hydrogen atoms were fixed geometrically at their calculated positions following riding atom model. The crystallographic data are listed in Table 1. Structural information has been deposited at the Cambridge Crystallographic Data Center (CCDC 1410686).

Table 1 Crystallographic data and structure refinement parameters for receptor **L**

Formula	C ₃₂ H ₃₀ N ₄ O ₆
Formula Weight	566.60
Crystal System	Monoclinic
Space group	P21/c
a [Å]	11.840(5)
b [Å]	10.520(5)
c [Å]	23.100(5)
β [°]	96.951(5)
V [Å ³]	2856.1(19)
Z	4
D(calc) [g/cm ³]	1.318
μ(MoKα) [/mm]	0.092
F(000)	1192
Crystal Size [mm]	0.14 x 0.16 x 0.20
Temperature (K)	293
Radiation [Å]	MoKα, 0.71073
Θ Min-Max [°]	2.1; 28.8
Dataset	-15: 15 ; -14: 14 ; -30: 30
Total Data	92134
Uniq. Data	7313
R(int)	0.168
Observed data [I > 2.0 sigma(I)]	3856
N _{ref}	7313
N _{par}	380
R	0.0963
wR ₂	0.2860
S	1.088

General method of UV-vis and fluorescence titrations

For UV-vis and fluorescence titrations, stock solution of the sensors **L** and [PbL₂]²⁺ were prepared (c = 1x10⁻⁵ ML⁻¹) in CH₃CN : H₂O (1 : 2, v/v). The solution of the guest metal

cations, anions and various amino acids were prepared ($c = 1 \times 10^{-4} \text{ ML}^{-1}$) in $\text{CH}_3\text{CN} : \text{H}_2\text{O}$ (1 : 2, v/v). The original volume of the receptor solutions are 3 mL each. Solutions of the sensors **L** and $[\text{PbL}_2]^{2+}$ of various concentrations and increasing concentrations of metal cations, anions and amino acids were prepared separately. The spectra of these solutions were recorded by means of UV-vis and fluorescence methods after mixing them for a few seconds at room temperature.

Colorimetric test kit

Chemosensors **L** and $[\text{PbL}_2]^{2+}$ (0.01 mmol) were dissolved in methanol (10 mL) to get 1mM solution. Test kits were prepared by immersing filter-papers into this solution (1 mM), and then dried in air to get rid of the solvent. Arginine and other amino acids were dissolved in water (10 mL) to prepare 0.1 mM solution. The test kits prepared above were dipped into the aqueous solution of arginine and other amino acids and then dried at room temperature.

Computational details

The GAUSSIAN-09 Revision C.01 program package was used for all calculations.⁴⁶ The gas phase geometries of the compounds **L** and $[\text{PbL}_2]^{2+}$ were fully optimized without any symmetry restrictions in singlet ground state with the gradient-corrected DFT level coupled with the hybrid exchange-correlation functional that uses Coulomb-attenuating method B3LYP.^{47,48} Basis sets 6-31G and LANL2DZ were found to be suitable for the molecule **L** and $[\text{PbL}_2]^{2+}$ respectively.

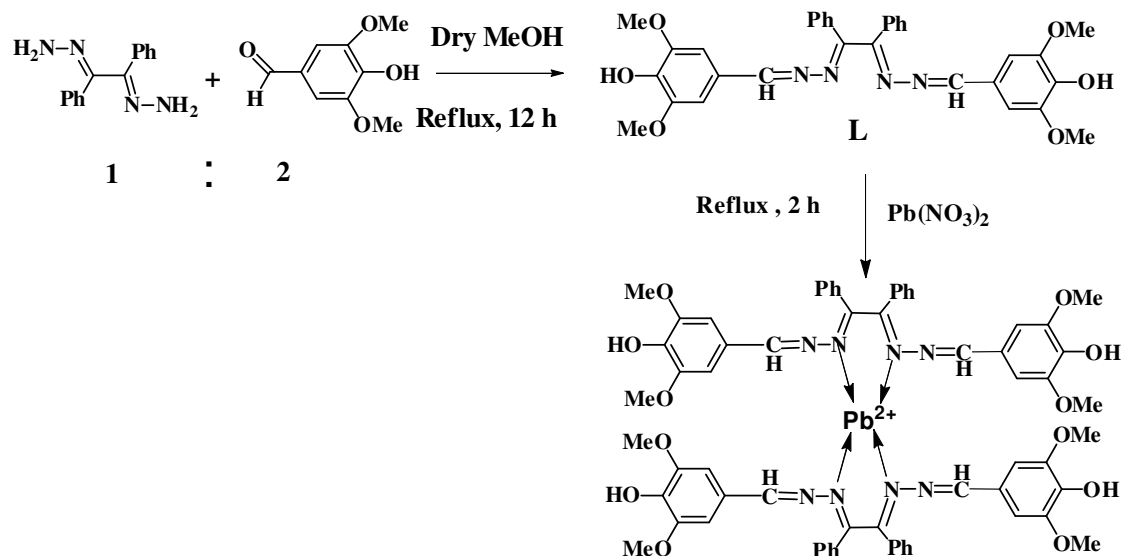
Result and discussion

Syntheses and structures of **L** and $[\text{PbL}_2]^{2+}$

Receptor **L** was obtained by the condensation reaction of benzil dihydrazone and syringaldehyde in methanol with 72% yield (Scheme 1) and characterized by ^1H NMR, ^{13}C NMR, IR, mass spectrometry, elemental analysis and X-ray crystallography and SEM imaging. The IR spectra of azino bis-Schiff base **L** showed a broad band at 3408 cm^{-1} for OH stretching vibration. In addition, the band appeared at 1597 cm^{-1} is due to $\gamma_{(\text{C}=\text{N})}$ stretching frequency.

$[\text{PbL}_2]^{2+}$ complex was obtained in good yield as a yellow solid by refluxing the mixture of the ligand **L** and $\text{Pb}(\text{NO}_3)_2$ in 2:1 molar proportion in methanol and it was characterized by IR, UV-Vis, HRMS-mass spectrometry, elemental analysis and SEM imaging. In the IR spectra the band appeared at 1310 cm^{-1} is due to $\gamma(\text{NO}_3^-)$ stretching

frequency. In SEM image studies framework like structure results due to strong interaction of the Pb^{2+} ion with the ligand **L** (Fig. S7).



Scheme 1 Synthetic procedure of the receptor **L** and PbL_2 .

To elucidate the structures of the chemosensors **L** and $[\text{PbL}_2]^{2+}$, we employed density functional theory (DFT) calculations using the Gaussian 09 software package. Chemosensors **L** and $[\text{PbL}_2]^{2+}$ were subjected to energy optimization using B3LYP/6-31G and B3LYP/LANL2DZ, respectively. The global minima structures for **L** and $[\text{PbL}_2]^{2+}$ are shown in Figs. 1 and 2 respectively. The optimized distance between the lead atom and the nitrogen atoms occupying 63, 64, 133 and 134 in $[\text{PbL}_2]^{2+}$ are 2.87, 2.75, 2.75 and 2.68 Å, respectively.

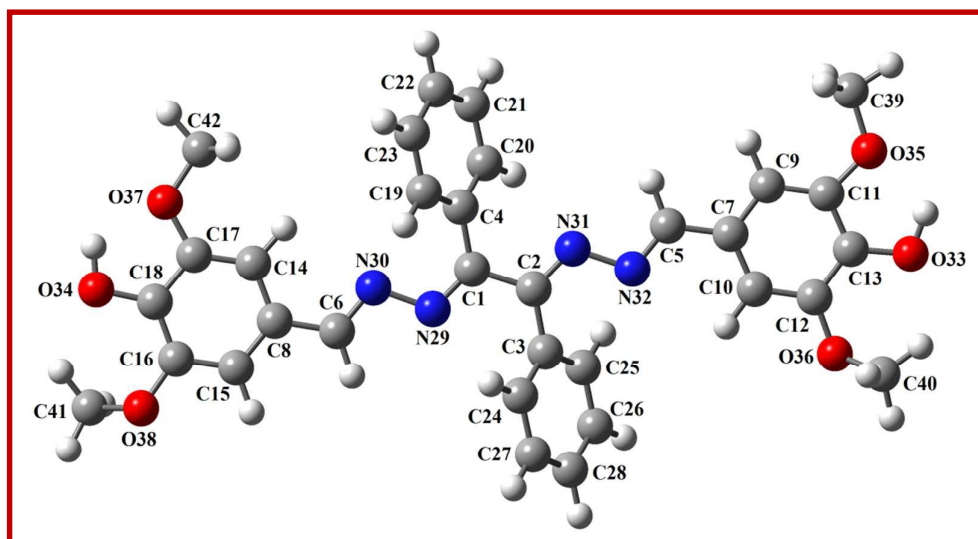


Fig. 1 Geometry optimized diagram of the molecule **L**

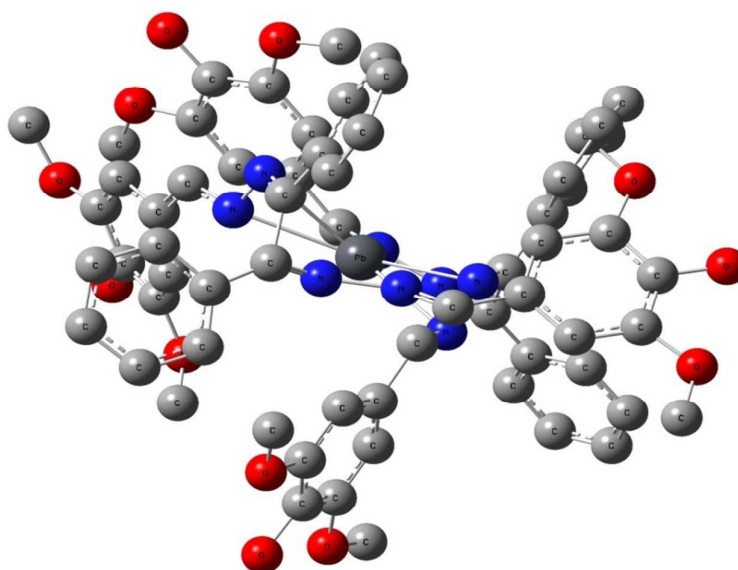


Fig. 2 DFT optimized structure of the $[\text{PbL}_2]^{2+}$. Hydrogen atoms are omitted for the sake of simplicity.

Crystals of **L** were obtained by slow evaporation of methanol solution. Single crystal-XRD analysis of **L** reveals that the molecule crystallizes in $P2_1/c$ space group and the 'z' value is 4. The ORTEP diagram of **L** is shown in Fig. 3. The molecular structure is based on the $-\text{C}^1-\text{N}^1-\text{N}^2-\text{C}^8-\text{C}^9-\text{N}^3-\text{N}^4-\text{C}^{10}-$ backbone where two unsubstituted phenyl rings are attached to the middle C-atoms (C^8 and C^9) and two substituted phenyl rings are attached to terminal C-atoms (C^1 and C^{10}). Even after numerous attempts we could not able to get single crystal of the $[\text{PbL}_2]^{2+}$ complex.

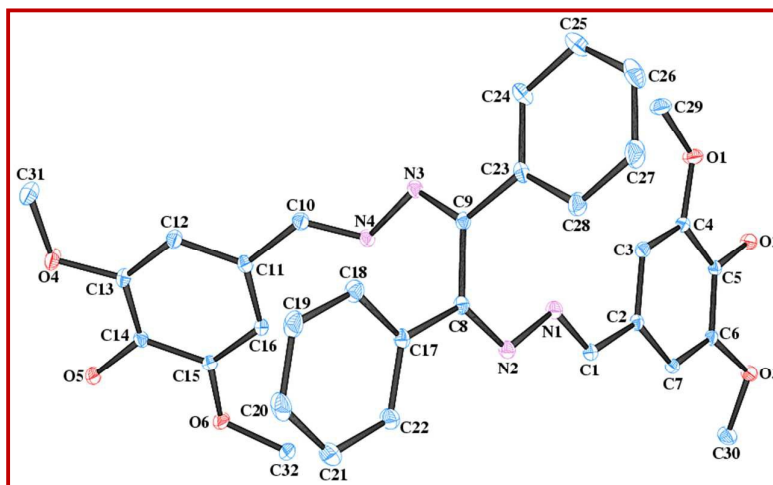


Fig. 3 ORTEP diagram of the **L** molecule (H atoms are omitted for clarity).

Absorption studies of **L** towards different amino acids

The photo-physical properties of probe **L** were investigated by monitoring the absorption behaviour with the addition of different analytes including competing amino acids (Gly, Ala, Lys, Trp, Arg, Val, His, Leu, Ph ala, Isoleu, Ser, Asp, Cys, Tyr and Glu), different metal cations and anions in solvent mixture of CH₃CN-H₂O (1:2, V/V). Only the addition of Arg induced distinct spectral changes while other amino acids did not induce any spectral change.

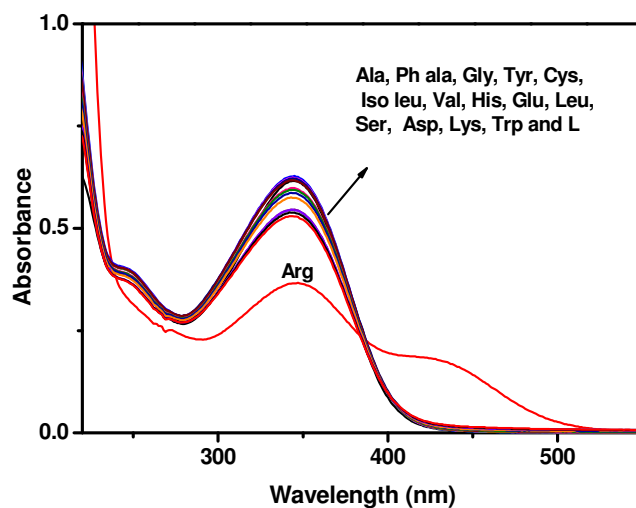


Fig.4 Changes in the absorption spectra of **L** (10 mM) in the presence of 10 eq. of different amino acids.

The probe **L** without Arg exhibited a strong UV-vis absorption band at 345 nm. Addition of arginine to a solution of **L** led to an obvious absorption enhancement at 430 nm with

concomitant decrease in absorption intensity at 345 nm (Fig. 4). Consistent with this change in the UV-Vis spectra, the solution of **L** resulted in an immediate colour change from colourless to yellow with the Arg (Fig. 5), indicating that receptor **L** can serve as a 'naked-eye' Arg indicator in aqueous solution.



Fig.5 The colour changes of **L** (10 μ M) upon addition of various amino acids (10 eq.) in $\text{CH}_3\text{CN-H}_2\text{O}$ (1:2, v/v) at room temperature.

The selectivity behaviour over a wide range of competing amino acids is obviously a matter of importance for an excellent sensing material. The exclusive selectivity of chemo-sensor **L** towards Arg was shown in bar graph (Fig. 6). However, the absorption study carried out with common metal cations and anions showed no significant change, indicating their non-interactive nature with **L** (Figs. S8 and S9). This indicates that under signalling conditions, the possible interference by them is not a practical problem in sensing of Arg by **L**.

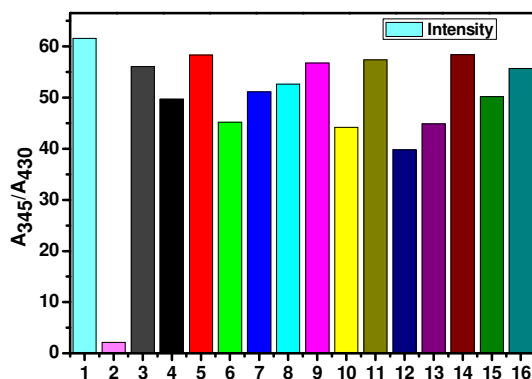


Fig. 6 The bar graph showing the relative absorption intensity of **L** upon treatment with various amino acids (1. **L**; 2. Arg; 3. Gly; 4. Ala; 5. Trp; 6. His; 7. Val; 8. Leu; 9. Ph ala; 10. Isoleu; 11. Ser; 12. Lys; 13. Asp; 14. Cys; 15. Tyr and 16. Glu).

The recognition ability of probe **L** towards Arg was established upon titration of the probe solution with variable concentration of Arg followed by subsequent measurement of absorption spectra (Fig. 7).

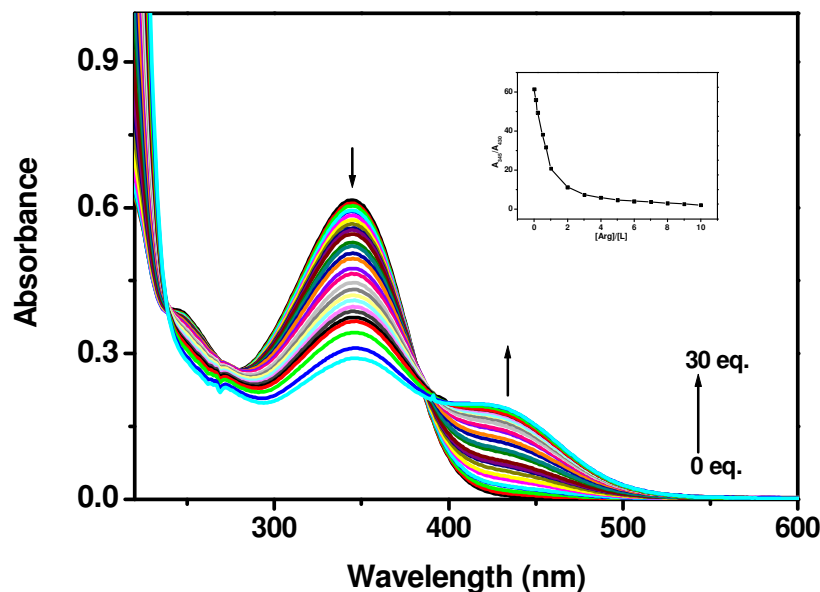


Fig. 7 Change in the absorption spectra of **L** after the addition of Arg up to 30 eq. (inset plot shows the change of relative intensity on addition of equivalence of Arg).

Interestingly, probe **L** exhibits two well-defined isosbestic points at 240 and 390 nm in the absorption spectra upon increasing concentration of Arg. In the UV–visible titration experiment, the blue-shifted band around 345 nm went down while the intensity of the newly formed band at 430 nm triggered by Arg continuously increases with successive increment of arginine (0–30 eq.) into the probe solution as shown in Fig. 7. The isosbestic point at 390 nm in the absorption spectra indicates an equilibrium between two species- the free ligand (colourless) and its deprotonated form (yellow). Among the 20 amino acids, arg with guanidino group has the highest pI value at about 10.8.^{49,50} Sensing of arg occurs here through the deprotonation of two terminal phenolic OH groups of the chemo-sensor by dint of the basic nature of Arg in aqueous solution. Though some cations are also basic in nature but as evidenced from UV spectra, Fig. S8 the receptors **L** is insensitive to these cations. At the concentration of measurements Arg is more basic than those cations. Upon the increasing amount of Arg, a new absorption band at lower energy (430 nm) appears which may led us to propose the transition of the intramolecular charge transfer (ICT) band through deprotonation of the chemo-sensor **L** by Arg, based on Bhattacharya's proposal.⁵¹⁻⁵³ To identify the ICT

Table 2 Absorption properties of **L** in various solvents

Solvent	$\lambda_{\text{abs}}[\text{nm}](\log\epsilon)$	$\lambda_{\text{em}}[\text{nm}]$
Methanol	345 (7.23)	430
Chloroform	352 (7.14)	436
Acetonitrile	347 (7.21)	440
DMSO	354 (7.11)	443

Fluorescence and absorption studies of $[\text{PbL}_2]^{2+}$ toward different amino acids

The ligand **L** employed is emission silent due to the photo-induced electron transfer (PET) transition in the molecule. But intense yellow coloured complex $[\text{PbL}_2]^{2+}$ in solvent mixture $\text{CH}_3\text{CN}-\text{H}_2\text{O}$ (2/1, v/v), was found to be strongly fluorescent upon excitation at 345 nm at room temperature. This is because of the fact that the presence of Pb^{2+} ion causes PET blocking through selective coordination to Pb^{2+} with the inner imino nitrogen atoms of **L**. In addition, the stable chelate formation of Pb^{2+} with **L** renders rigidity to the resulting complex thereby generating efficient chelation enhanced fluorescence (CHEF). The fluorescence response of $[\text{PbL}_2]^{2+}$ complex towards above-mentioned amino acids were investigated in acetonitrile-water (2/1, v/v) as shown in Fig. 9. It was observed that the fluorescence emission at 442 nm completely disappeared after the addition of Arg. Under the same condition, the addition of the other amino acids caused small decrease in fluorescence intensity with hardly perceptible colour changes of the solution.

Only Lys has some influence in quenching of fluorescence emission of the solution of complex albeit negligible in comparison to that observed in case of Arg (Fig. 10). These results indicated that the presence of other amino acids including Lys did not obviously affect the Arg detection under the same experimental condition.

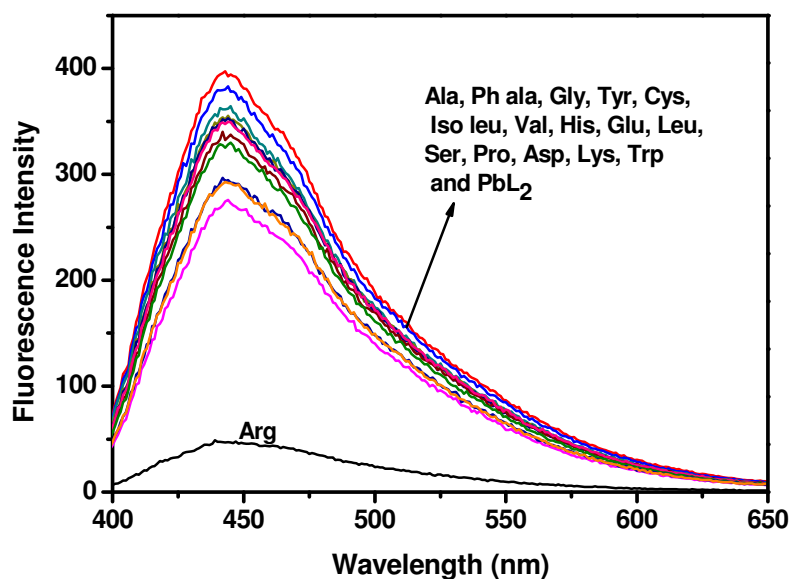


Fig. 9 Fluorescence spectra of $[\text{PbL}_2]^{2+}$ complex ($10 \mu\text{M}$) before and after addition of various amino acids (10 eq.).

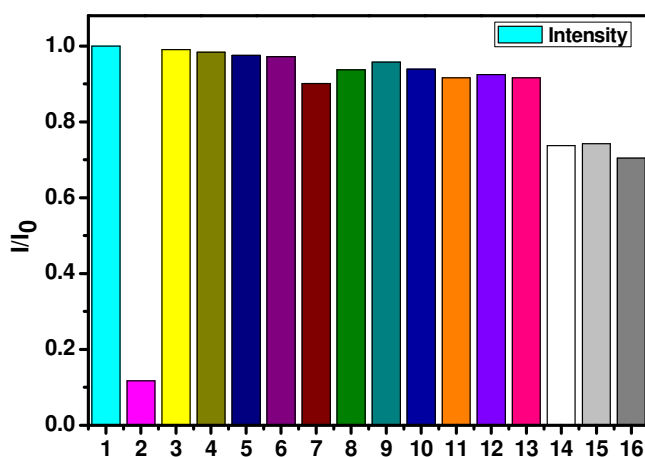


Fig. 10 The bar graph showing the relative fluorescence intensity of $[\text{PbL}_2]^{2+}$ upon treatment with various amino acids (1. $[\text{PbL}_2]^{2+}$; 2. Arg; 3. Gly; 4. Ala; 5. Trp; 6. Cys; 7. Val; 8. Leu; 9. Ph ala; 10. Isoleu; 11. Ser; 12. Glu; 13. Asp; 14. His; 15. Tyr and 16. Lys).

Sensitivity is an important criterion for the fluorescence sensor. To study the sensitivity of the chemo-sensor $[\text{PbL}_2]^{2+}$ with respect to Arg, the probe was titrated by varying the concentration of Arg in aqueous solution. Upon gradual addition of Arg, the

fluorescence intensity of the complex gets decreased gradually. The fluorescence changes of $[\text{PbL}_2]^{2+}$ upon addition of Arg is shown in Fig. 11. The inset picture in Fig. 11 which depicts the relationship between the relative fluorescence intensity (I/I_0) and Arg concentration shows good linearity (linearly dependent coefficient $R^2 = 0.987$) in low concentration range (0 - 2 μM) which was over the Arg concentration range of $0.6 - 0.8 \times 10^{-4} \text{ mol L}^{-1}$ in healthy body plasma samples.⁵⁶ This demonstrates the potential application of $[\text{PbL}_2]^{2+}$ complex as an efficient indicator which shows the plasma sample is healthy or not. From the titration profile the detection limit calculated is 0.1 nM (Fig. S12b).

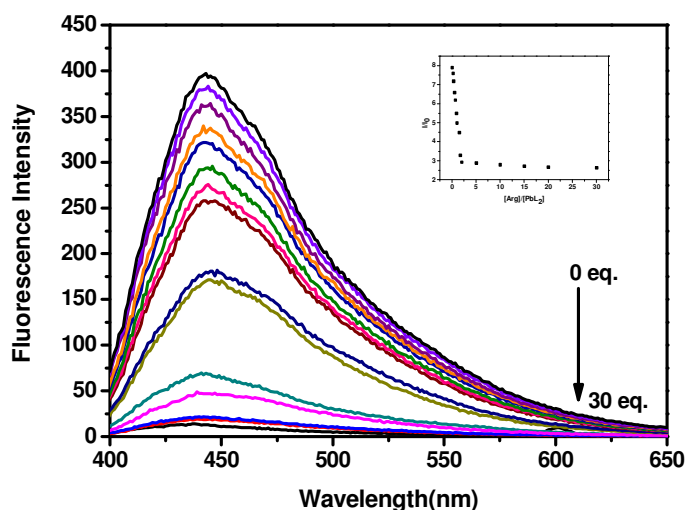


Fig. 11 Change in the fluorescence spectra of $[\text{PbL}_2]^{2+}$ after the addition of Arg upto 30 eq. (inset plot shows the change of relative intensity on addition of equivalence of Arg).

To further investigate the selectivity of the $[\text{PbL}_2]^{2+}$ towards Arg, the possible interferences by other amino acids were also conducted through competitive experiments in aqueous media. The fluorescence emission intensity of $[\text{PbL}_2]^{2+}$ complex in acetonitrile-water (2/1, v/v) were monitored after adding 10 eq. of Arg and other interfering amino acids, as shown in Fig. 12. Under the same concentration, the tested interfering analytes showed no obvious interference to the detection of Arg except His and Lys showing only a little interference. The response of $[\text{PbL}_2]^{2+}$ complex toward the interfering analytes revealed a high selectivity to Arg against other analytes under the same conditions.

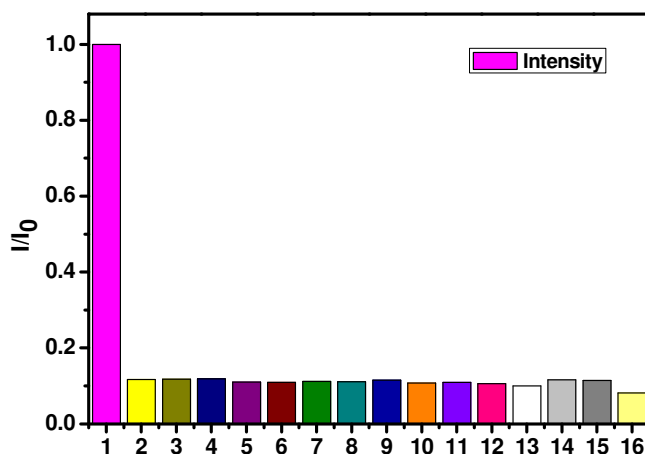


Fig.12 Competitive experiment in presence of other amino acids (1. [PbL₂]²⁺; 2. [PbL₂]²⁺ + Arg; 3. [PbL₂]²⁺ + Arg + Gly; 4. [PbL₂]²⁺ + Arg + Ala; 5. [PbL₂]²⁺ + Arg + Trp; 6. [PbL₂]²⁺ + Arg + Cys; 7. [PbL₂]²⁺ + Arg + Val; 8. [PbL₂]²⁺ + Arg + Leu; 9. [PbL₂]²⁺ + Arg + Ph ala; 10. [PbL₂]²⁺ + Arg + Isoleu; 11. [PbL₂]²⁺ + Arg + Ser; 12. [PbL₂]²⁺ + Arg + Glu; 13. [PbL₂]²⁺ + Arg + His; 14. [PbL₂]²⁺ + Arg + Asp; 15. [PbL₂]²⁺ + Arg + Tyr and 16. [PbL₂]²⁺ + Arg + Lys).

The results obtained in the entire fluorescence spectra are well consistent with the UV-visible spectral behaviour of [PbL₂]²⁺ complex towards Arg. The colorimetric selective sensing abilities of complex [PbL₂]²⁺ with various amino acids in a mixture of CH₃CN–H₂O (2: 1, v/v) were also investigated by UV-Vis absorption spectrometry (Fig.S13).

Only the addition of Arg induced distinct spectral changes while other amino acids did not induce any spectral changes. A UV-visible spectrometric titration of [PbL₂]²⁺ in acetonitrile-water (2/1, v/v) with aqueous solution of Arg revealed that the absorption band at 380 nm decreased and two new bands at 290 nm and 450 nm emerged resulting an isosbestic point at 415 nm (Fig.13) with an immediate colour change from yellow to colourless (inset picture of Fig. 13).

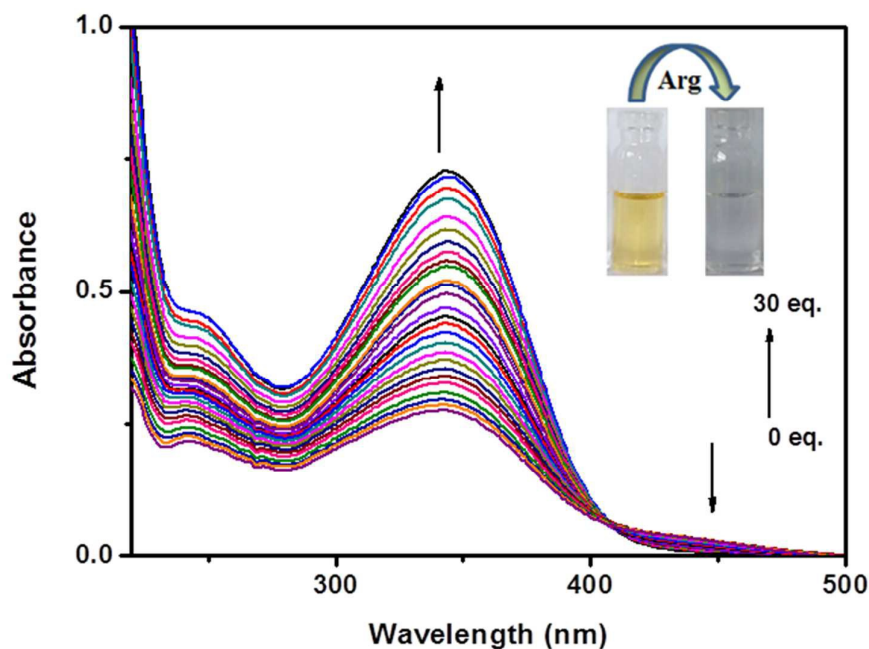
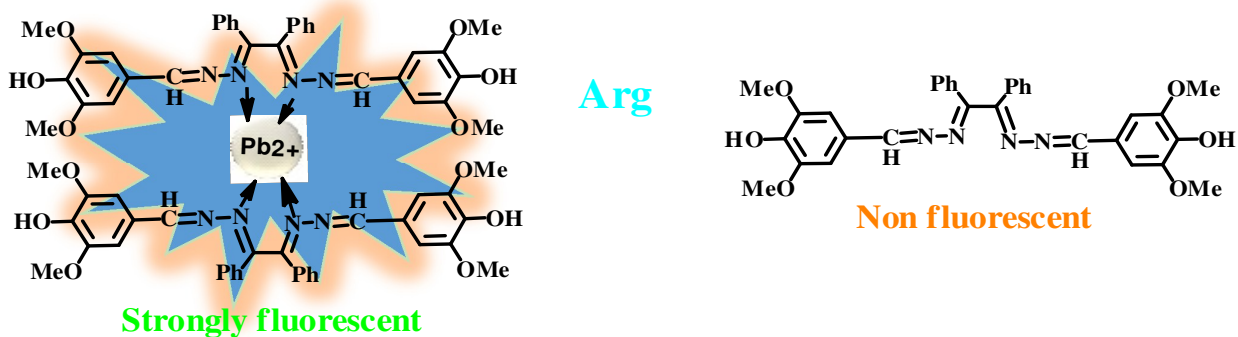


Fig. 13 Change in the absorption spectra of $[\text{PbL}_2]^{2+}$ after the addition of Arg up to 30 eq. (inset plot shows the colour change on addition of Arg).

Sensing mechanism of $[\text{PbL}_2]^{2+}$

$[\text{PbL}_2]^{2+}$ complex in acetonitrile-water (2/1, v/v) shows amplified fluorescence owing to hindered PET and CHEF effect. Subsequently, when Arg was added into the $[\text{PbL}_2]^{2+}$ complex solution, the interactions of its stronger alkaline centres with Pb^{2+} promoted the dissociation of $[\text{PbL}_2]^{2+}$ complex and thereby produced the free ligand L (Scheme 2).



Scheme 2 Sensing mechanism of $[\text{PbL}_2]^{2+}$

This resulted in the quenching of fluorescence intensity. In order to obtain better insight into the sensing mechanism, mass spectral studies of $[\text{PbL}_2]^{2+}$ complex have been carried out after addition of Arg. This study stands in support of regeneration of free ligand L

in sensing mechanism, which is confirmed by the appearance of a peak at m/z 567, assignable to $[L+H]^+$ in the ESI/MS (Fig. 14).

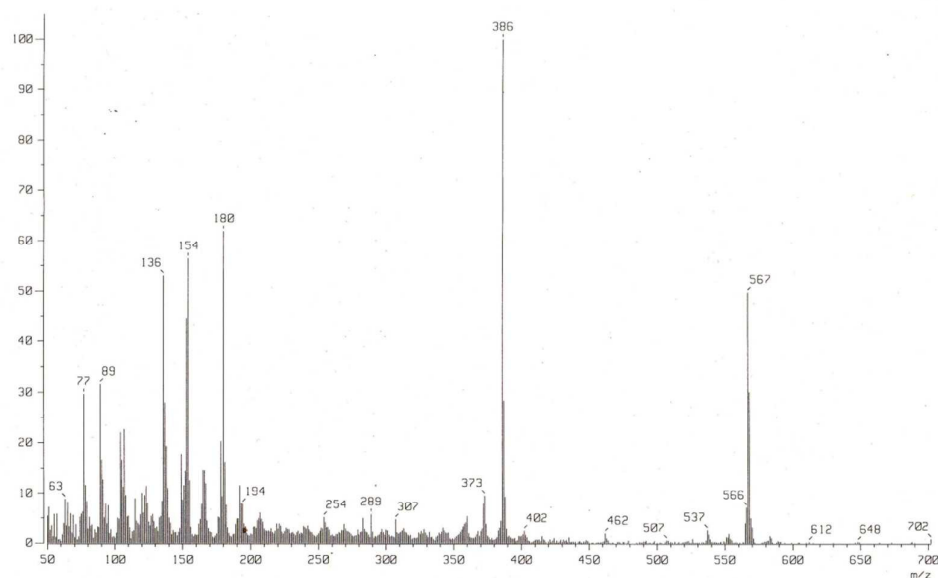


Fig.14 Mass Spectra of $[PbL_2]^{2+}$ after addition of Arg.

The quick response time for a sensing material is a prerequisite for practical applicability. To understand the dissociation time of $[PbL_2]^{2+}$ complex in presence of Arg, the fluorescence spectra of probe $[PbL_2]^{2+}$ complex was recorded by variable time interval and the results revealed that the response of change in fluorescence intensity started immediately upon addition Arg and almost completed within 1 min as shown in the fluorescence spectra at different time intervals (Fig. 15). It was observed that fluorescence intensity remained almost constant up to 15 min on addition of 10 eq. of Arg.

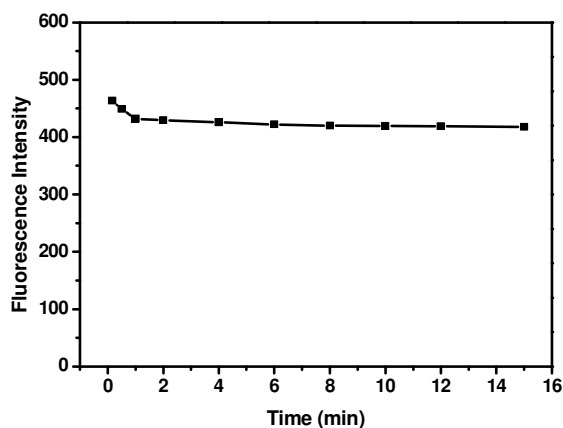


Fig.15 Time evolution of for Arg.

Application of chemosensor **L**

To check the practical application, the test kits were utilized to sense Arg among different competing amino acids. As shown in Fig. 16, when the test kits coated with **L** were added to aqueous solution of different amino acids, the obvious colour change was observed only with Arg. Therefore, the test kits coated with the chemo-sensor **L** solution would be convenient for detecting Arg. These results showed that chemo-sensor **L** could be a valuable practical sensor for environmental analyses of Arg. For practical application of the $[\text{PbL}_2]^{2+}$ we have performed similar type colorimetric test kit experiment. But it has been found that the $[\text{PbL}_2]^{2+}$ solution cannot stain the filter paper.

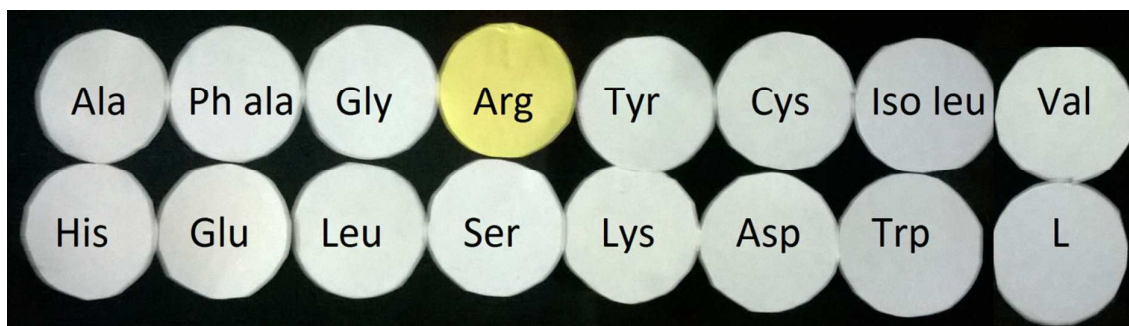


Fig. 16 Photographs of the test kits with **L** (0.5 mM) for detecting Arg among other amino acids.

Conclusion

In this work, we have synthesized a novel, exceptionally simple and cost effective bis Schiff base ligand **L** and its Pb^{2+} -complex, $[\text{PbL}_2]^{2+}$ and exploited them for expeditious detection of arginine. The ligand can be successfully applied as a colorimetric sensor for arginine detection whereas $[\text{PbL}_2]^{2+}$ has the potential to detect arginine in fluorescent-colorimetric way. Both the chemo-sensors exhibit excellent selectivity and sensitivity towards arginine in aqueous solution. The detection limits calculated $0.67 \mu\text{M}$ (for **L**) and 0.1 nM (for $[\text{PbL}_2]^{2+}$) are fairly below in comparison to those found in literature. To the best of our knowledge, this is the first time to report a simple Schiff base and its metal complex acting as an efficient chemo-sensor for Arg.

Acknowledgements

G.K.P would like to thank the Department of Science and Technology and Department of Biotechnology, Government of India, New Delhi for financial support and Dr. Pathik Maji for various help.

References

1. G. Coruzzi and D. R. Bush, *Plant Physiol*, 2001, **125**, 61–64.
2. M.A. Vermeulen, M.C. van de Poll, G.C. Ligthart-Melis, C.H. Dejong, M.P. van den Tol, P.G. Boelens and P.A. van Leeuwen, *Crit. Care Med.*, 2007, **35**, S568–S576.
3. H. Tapiero, G. Mathé, P. Couvreur and K.D. Tew, *Biomed. Pharmacother*, 2002, **56**, 439–445.
4. J.K. Stechmiller, B. Childress and L. Cowan, *Nutr. Clin. Pract.*, 2005, **20**, 52–61.
5. M.B. Witte and A. Barbul, *Wound Repair Regen.* 2003, **11**, 419–423.
6. N. Guelzim, F. Mariotti, P.G.P. Martin, F. Lasserre, T. Pineau and D. Hermier, *Amino Acids*, 2011, **41**, 969–979.
7. M.M. Nascimento, V.V. Gordan, C.W. Garvan, C.M. Browngardt and R.A. Burne, *Microbiol. Immun.* 2009, **24**, 89–95.
8. F. Wimmer, T. Oberwinkler, B. Bisle, J. Tittor and D. Oesterhelt, *FEBS Lett.*, 2008, **582**, 3771–3775.
9. Y. Fang, T. Shane, F. Wu, C. Williams and C. Miller, *Biophys. J.*, 2010, **98**, 418–426.
10. S.M. Morris, D. Loscalzo, W.W. Bier and J. Souba, *J. Nutr.*, 2004, **134**, 2741S–2897S.
11. G. Wu, F.W. Bazer, T.A. Davis, S.W. Kim, P. Li, J.M. Rhoads, M.C. Satterfield, S.B. Smith, T.E. Spencer and Y. Yin, *Amino Acid*, 2009, **37**, 153–168.
12. A.W. Deckel, P. Volmer, R. Weiner, K.A. Gary, J. Covault, D. Sasso, N. Schmerler, D. Watts, Z. Yan and I. Abeles, *Brain Res.*, 2000, **875**, 187–195.
13. R.R. Julian and J.L. Beauchamp, *Int. J. Mass. Spectrom.*, 2001, **210**, 613–623.
14. R.R. Julian, M. Akin, J.A. May, B.M. Stoltz and J.L. Beauchamp, *Int. J. Mass. Spectrom.* 2002, **220**, 87–96.
15. V. Gopalakrishnan, P.J. Burton and T.F. Blaschke, *Anal. Chem.*, 1996, **68**, 3520–3523.
16. H. Chen, L. Gu, Y. Yin, K. Koh and J. Lee, *Int. J. Mol. Sci.*, 2011, **12**, 2315–2324.
17. K. Vishwanathan, R.L. Tackett, J.T. Stewart and M.G. Bartlett, *J. Chromatogr. B*, 2000, **748**, 157–166.
18. A. Alonso, M.J. Almendral, M.D. Baez, M.J. Porras and C. Alonso, *Anal. Chim. Acta* 1995, **308**, 164–169.
19. K.-M. Chu, P.-W. Huang and L.-H. Pao, *J. Med. Sci.*, 2003, **23**, 201–206.
20. J. Costin, F. Paul and S. Lewis, *Anal. Chim. Acta*, 2003, **408**, 67–77.
21. J.M. Lobenhoffer, O. Krug and S.M. Bode-Bogerh, *J. Mass Spectrom.*, 2004, **39**, 1287–1294.

22. G.A. Rechnitz, R.K. Kobos, S.J. Riechel and C.R. Gebauer, *Anal. Chim. Acta*, 1977, **94**, 357–365.
23. S.R. Grobler, N. Basson and C.W. van Wyk, *Talanta*, 1982, **29**, 49–51.
24. D.P. Nikolelis and T.P. Hadjiioannou, *Anal. Chim. Acta.*, 1983, **147**, 33–39.
25. S. Karacaoglu and S. Timur, *Cells Blood Subst. Immob. Biotechnol.*, 2003, **31**, 357–363.
26. R. Koncki, I. Walcerz, F. Ruckruh and S. Glab, *Artif. Cells Blood Subst. Immob. Biotechnol.*, 1996, **333**, 215–222.
27. X. Chen, T. Pradhan, F. Wang, J.S. Kim, J. Yoon, *Chem. Rev.*, 2012, **112**, 1910–1956.
28. M. Zhang, M. Yu, F. Li, M. Zhu, M. Li, Y. Gao, L. Li, Z. Liu, J. Zhang, D. Zhang, T. Yi, C. Huang, *J. Am. Chem. Soc.*, 2007, **129**, 10322–10323.
29. S. Kaur, V. Bhalla, M. Kumar, *Chem. Commun.*, 2014, **50**, 9725–9728.
30. T. Anand, G. Sivaraman, D. Chellappa, *J. Photochem. Photobio. A*, 2014, **281**, 47–52.
31. J. Du, Z. Huang, X.-Q. Yu, L. Pu, *Chem. Commun.*, 2013, **49**, 5399–5401.
32. X. Wang, Q. Miao, T. Song, Q. Yuan, J. Gao, G. Liang, *Analyst*, 2014, **139**, 3360–3364.
33. Y. Hu, C.H. Heo, G. Kim, E.J. Jun, J. Yin, H.M. Kim, J. Yoon, *Anal. Chem.*, 2015, **87**, 3308–3313.
34. D.R. Mishra, S.M. Darjee, K.D. Bhatt, K.M. Modi, V.K. Jain, *J. Incl. Phenom. Macrocycl. Chem.*, (2015) DOI: 10.1007/s10847-10015-10509-10848.
35. Ying Zhou, Jiyeon Won, Jin Yong Lee and Juyoung Yoon, *Chem. Commun.*, 2011, **47**, 1997–1999.
36. A. Buryak, K. Severin, *J. Am. Chem. Soc.*, 2005, **127**, 3700–3701.
37. Tsuyoshi Minami, Nina A. Esipenko, Ben Zhang, Lyle Isaacs and Pavel Anzenbacher, Jr, *Chem. Commun.*, 2014, **50**, 61–63.
38. Mark Wehner, Thomas Schrader, Paolo Finocchiaro, Salvatore Failla and Giuseppe Consiglio, *Org. Lett.*, 2000, **2**, 605–608.
39. Jianhua Cao, Liping Ding, Yuanyuan Zhang, Shihuai Wang, Yu Fang, *Journal of Photochemistry and Photobiology A: Chemistry*, 2016, **314**, 66–74.
40. Wendan Pu, Huawen Zhao, Chengzhi Huang, Liping Wu, Dan Xu, *Analytica Chimica Acta*, 2013, **764**, 78–83
41. A. Ghorai, J. Mondal, R. Chandra and G. K. Patra, *Dalton Trans.*, 2015, **44**, 13261–13271.
42. A. Ghorai, J. Mondal, R. Chandra and G. K. Patra, *Analytical Methods*, 2015, **7**, 8146–8151.

43. *SMART & SAINT Software Reference manuals, version 5.0; Bruker AXS Inc.:* Madison, WI, 1998.
44. T. Gruene, H. W. Hahn, A. V. Luebben, F. Meilleur and G. M. Sheldrick, *J. Appl. Cryst.*, 2014, **47**, 462-466.
45. L.J. Farrugia, *WinGX: An Integrated System of Windows Programs for the Solution, Refinement and Analysis for Single Crystal X-ray Diffraction Data, version 1.80.01;* Department of Chemistry: University of Glasgow, 2003. *J. Appl. Crystallogr.*, 1999, 32837.
46. M.J. Frisch, G.W. Trucks, H.B. Schlegel, G.E. Scuseria, M.A. Robb, J.R. Cheeseman, G. Scalmani, V. Barone, B. Mennucci, G.A. Petersson, H. Nakatsuji, M. Caricato, X. Li, H. P. Hratchian, A. F. Izmaylov, J. Bloino, G. Zheng, J. L. Sonnenberg, M. Hada, M. Ehara, K. Toyota, R. Fukuda, J. Hasegawa, M. Ishida, T. Nakajima, Y. Honda, O. Kitao, H. Nakai, T. Vreven, J. A. Montgomery, Jr., J.E. Peralta, F. Ogliaro, M. Bearpark, J. J. Heyd, E. Brothers, K. N. Kudin, V. N. Staroverov, R. Kobayashi, J. Normand, K. Raghavachari, A. Rendell, J. C. Burant, S. S. Iyengar, J. Tomasi, M. Cossi, N. Rega, J. M. Millam, M. Klene, J. E. Knox, J. B. Cross, V. Bakken, C. Adamo, J. Jaramillo, R. Gomperts, R. E. Stratmann, O. Yazyev, A. J. Austin, R. Cammi, C. Pomelli, J.W. Ochterski, R. L. Martin, K. Morokuma, V.G. Zakrzewski, G.A. Voth, P. Salvador, J. J. Dannenberg, S. Dapprich, A. D. Daniels, Ö. Farkas, J. B. Foresman, J.V. Ortiz, J. Cioslowski, and D. J. Fox. *Gaussian 09, Revision C.01, Gaussian Inc.*, Wallingford, CT, 2009.
47. A.D. Becke, *J. Chem. Phys.*, 1993, **98**, 5648-5652.
48. C. Lee, W. Yang and R.G. Parr., *Phys. Rev. Sect. B*, 1988, **37**, 785-789.
49. L.Pogliani, *J. Pharm. Sci.*, 1992, **81**,334-336.
50. H. Cohen, A. Gedanken, Z. Zhong, *J. Phys. Chem. C.*, 2008, **112**, 15429-15438.
51. N. Kumari, S. Jha and S. Bhattacharya, *J. Org. Chem.*, 2011,**76**, 8215–8222.
52. L. Li, F. Liu and H. Li, *Spectrochim. Acta, Part A*, 2011, **79**, 1688–1692
53. P. Xie, F. Guo, S. Yang, D. Yao, G. Yang and L. Xie, *J. Fluoresc.*, 2014, **24**, 473-480
54. S. Maruyama, K. Kikuchi, T. Hirano, Y. Urano, T. Nagano and A. Novel, *J. Am. Chem. Soc.*, 2002, **124**, 10650–10651.
55. S. Park, K. Hong, J. Hong and H. Kim, *Sens. Actuators, B*, 2012, **174**, 140-144
56. J. Martens-Lobenhoffer, S.M. Bode-Böger, *Eur. J.Clin. Pharmacol.* 2006, **62**, 61–68.

GRAPHICAL ABSTRACT

A new Schiff base and its metal complex as a fluorescent-colorimetric sensor for rapid detection of arginine

Anupam Ghorai, Jahangir Mondal and Goutam K Patra*

Department of Chemistry, Guru Ghasidas Vishwavidyalaya, Bilaspur (C.G)

A new Schiff base and its Pb^{2+} -complex have been utilized, for the first time, for the detection of arginine in aqueous medium. Receptor **L** exhibits an excellent selective colorimetric response towards arginine whereas Pb^{2+} -complex has been exploited as a highly selective fluorescent-colorimetric probe for rapid detection of arginine. The sensitivity of the fluorescent based assay for arginine is sufficiently low (0.1 nM). The geometry of **L** has been optimized both by DFT calculation and single crystal X-ray studies.

